Tetrahedron Letters 52 (2011) 2181–2184

Contents lists available at ScienceDirect

Tetrahedron Letters

journal homepage: www.elsevier.com/locate/tetlet

Entropy versus tether strain effects on rates of intramolecular 1,3-dipolar cycloadditions of *N*-alkenylnitrones

Elizabeth H. Krenske [a,b,c,*], K. N. Houk [c,*], Andrew B. Holmes [a,d], John Thompson [e]

[a] School of Chemistry, The University of Melbourne, Vic. 3010, Australia
[b] Australian Research Council Centre of Excellence for Free Radical Chemistry and Biotechnology, Australia
[c] Department of Chemistry and Biochemistry, University of California, Los Angeles, CA 90095, USA
[d] CSIRO, Materials Science and Engineering, Bayview Avenue, Clayton Vic. 3168, Australia
[e] Department of Chemistry, University of Cambridge, Lensfield Road, Cambridge CB2 1EW, UK

ARTICLE INFO

Article history:
Available online 29 November 2010

Dedicated to Harry H. Wasserman on the occasion of his 90th birthday

Keywords:
Nitrone
1,3-Dipolar cycloaddition
Density functional calculations
Transition states
Ring strain

ABSTRACT

Intramolecular 1,3-dipolar cycloadditions of two *N*-alkenylnitrones are studied by means of density functional theory calculations. Cycloaddition of an acyclic 4-hexenylnitrone led to the expected isoxazolidine in 46% yield, but a 4-cycloheptenylnitrone did not react. Calculations of the transition states for cycloaddition indicate that although the cycloheptenyl nitrone has a more favorable activation entropy, the strain associated with distortion of the tethering groups into the required boat conformation disfavors the reaction of the cyclic substrate over the acyclic substrate by 8.7 kcal/mol.

Intramolecular 1,3-dipolar cycloadditions of nitrones with alkenes have been employed in many natural product syntheses.[1–3] During the studies of the synthesis of carpamic acid (**4**) (Scheme 1), we employed the intramolecular cycloaddition of the 4-hexenyl nitrone **2**, which furnished the isoxazolidine **3** in an overall yield of 46% based on oxime **1**.[4] In contrast, efforts to bring about the intramolecular cycloaddition of the related cycloheptenyl nitrone **5** failed to produce any of the expected cycloadduct **6**. A similar lack of reactivity was observed in an analogous system when the alkene was contained in a 16- rather than a seven-membered ring. The reason for the difference in reactivity between acyclic **2** and cyclic **5** was not obvious, since the tethering of both termini of the dipolarophile units in **5** might have been thought to provide an additional entropic advantage. We have undertaken a computational study to uncover the origin of this disparity.

Density functional theory calculations at the B3LYP/6-31G(d) level were performed in GAUSSIAN 03.[5] Previous theoretical studies[6] of the mechanisms and regioselectivities of nitrone 1,3-dipolar cycloadditions have shown that these are usually concerted processes.

To quantify the effect of the alkene configurations in **2** and **5**, transition states were first calculated for the cycloaddition of

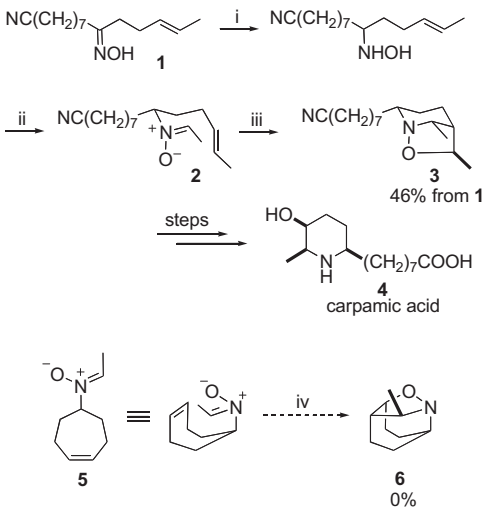

Scheme 1. 1,3-Dipolar cycloaddition approaches to carpamic acid. Reagents and conditions: (i) $NaCNBH_3$, HCl; (ii) MeCHO, Na_2SO_4; (iii) toluene, reflux; 46% from **1**; (iv) benzene (40–80 °C) or toluene (110–115 °C) or *t*-amyl alcohol (115 °C).

* Corresponding authors. Tel.: +61 3 8344 0080; fax: +61 3 9347 8189 (E.H.K.); tel.: +1 310 206 0515; fax: +1 310 206 1843 (K.N.H.).
E-mail addresses: ekrenske@unimelb.edu.au (E.H. Krenske), houk@chem.ucla.edu (K.N. Houk).

0040-4039/$ - see front matter © 2010 Elsevier Ltd. All rights reserved.
doi:10.1016/j.tetlet.2010.11.121

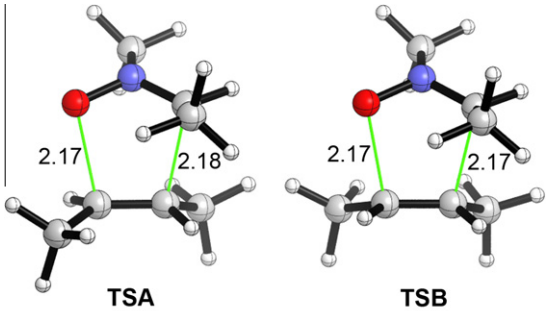

Figure 1. Calculated transition structures for the cycloadditions of *N*-methyl-*C*-methylnitrone with *trans*- and *cis*-2-butene. Bond distances in Å, activation energies in kcal/mol at 298.15 K.

N-methyl-*C*-methylnitrone with *trans*- and *cis*-2-butene.[7] The TS geometries are shown in Figure 1. The configuration of the alkene has little effect on either the geometry of the TS or the activation energy. Both alkenes react via synchronous transition states, and the activation barrier for the *cis* alkene (**TSB**) is 0.6 kcal/mol higher than that for the *trans* alkene (**TSA**). This greater reactivity of *trans* alkenes was previously noted by Huisgen.[8]

Transition structures for the intramolecular cycloadditions of **2** and **5** are shown in Figure 2. The acyclic *N*-alkenylnitrone **2** was modeled by the methyl analog **7**.

Both of the intramolecular TSs are less synchronous than the intermolecular ones: the forming C–C bonds are shorter than the forming C–O bonds, and this asynchronicity is more pronounced in **TSC** than in **TSD**. In **TSC**, the forming six-membered ring adopts a chair conformation. Other conformers were at least 2.9 kcal/mol higher in energy. The two forming six-membered rings in **TSD** are by contrast necessarily boats, and the cycloheptene ring is also forced to adopt a boat conformation. Consequently, there are significant eclipsing interactions along each C–C bond in the tethers.

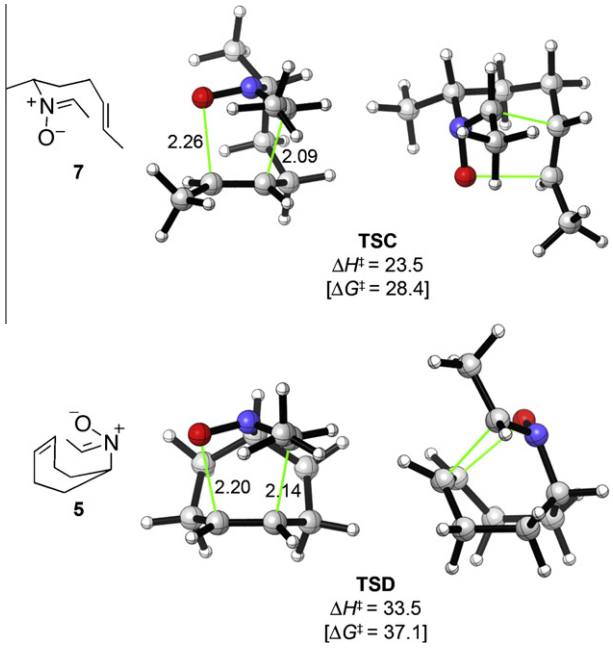

Figure 2. Two views of the calculated transition structures for the intramolecular 1,3-dipolar cycloadditions of the acyclic *N*-alkenylnitrone **7** and the *N*-cycloalkenylnitrone **5**.

The activation enthalpy for **TSC** (23.5 kcal/mol) is only 2.1 kcal/mol higher than that of the corresponding intermolecular cycloaddition (**TSA**), and its free energy of activation (28.4 kcal/mol) is 6.9 kcal/mol lower. Intramolecularity in this case produces an entropic advantage. The entropies of activation are −46.7 e.u. for **TSA** and −16.5 e.u. for **TSC**.

The activation enthalpy for **TSD** (33.5 kcal/mol) is 11.5 kcal/mol higher than the intermolecular analog, **TSB**. The free energy of activation is 1.2 kcal/mol higher than the intermolecular value. Here, the values of $\Delta S^{\ddagger}$ are −46.5 e.u. for **TSB** and −12.0 e.u. for **TSD**. The 8.7 kcal/mol difference in $\Delta G^{\ddagger}$ between **TSC** and **TSD** is consistent with the failure of **5** to undergo intramolecular cycloaddition under the experimental conditions.

Similar results are obtained with use of the M06-2X functional.[9,10] Single-point energy calculations at the M06-2X/6-311+G(d,p) level on the B3LYP geometries gave activation enthalpies for **TSC** and **TSD** of 22.9 and 33.4 kcal/mol, respectively ($\Delta H^{\ddagger}_{OK}$).[11] Details are provided in the Supplementary data.

To account for the difference in barriers, we computed the energies associated with distorting various fragments of the substrates **7** and **5** into the geometries observed in **TSC** and **TSD**. The analysis is shown in Figure 3, where the transition structures are reproduced on the left. In the center (**C-1** and **D-1**), the atoms connecting the nitrone to the alkene (2-butenyl fragment) have been removed and replaced by H's, to provide an estimate of the distortion energies within the five-membered bond-forming array alone. On the right (**C-2** and **D-2**), the nitrone group has been replaced by NH_2 and the remainder of the structure held fixed, to provide an estimate of the energy associated with distorting the tether to the geometry in the TS. The bond lengths, angles, and dihedrals of the added H atoms were allowed to relax, while all other structural features were held at the same values as in **TSC** or **TSD**.[12]

Comparison of structures **C-1** and **D-1** indicates that the distortions of the nitrone and alkene to their TS geometries are more difficult for **TSD**, but the difference is minor: ΔE_{dist}(nitrone)‡ and ΔE_{dist}(alkene)‡ are only 0.5 and 1.1 kcal/mol higher for **TSD** than for **TSC**, respectively. A greater contribution to the difference in barriers arises from the different orientation (dihedral angle) of the nitrone with respect to the alkene in **TSC** and **TSD**. The less-favorable overlap between the nitrone and the alkene in **TSD** leads to a less stabilizing interaction between these two components: $\Delta E^{\ddagger}_{int}$ is 3.6 kcal/mol less favorable in **TSD** than in **TSC**. However, the major factor that destabilizes **TSD** is the conformation of the tether connecting the nitrone to the alkene. Distortion of cycloheptenylamine to a geometry like that found in **D-2** requires some 35.7 kcal/mol, whereas distortion of the hexenylamine to the geometry found in **C-2** requires only 27.9 kcal/mol. The difference between these values, 8 kcal/mol, is a substantial part of the activation energy difference.

The distortion of the cycloheptene ring required to achieve the TS is evident also in the conformational preferences of the reactant nitrone. In Figure 4 are shown the lowest-energy chair and boat conformers of **5**. The chair conformation is preferred by 4.3 kcal/mol. The distorted boat in **TSD** is even more difficult to access than the boat reactant.

Intramolecular cycloaddition of a related *N*-alkenylnitrone containing a cyclohexenyl group (**8**, Scheme 2) was reported by Oppolzer.[13] The *N*-cyclohexenylmethylnitrone **8** furnished the cycloadduct **9** in 64% yield. The transition structure for this transformation (**TSE**) and activation barriers are shown below. The newly-forming six- and seven-membered rings in **TSE** both adopt chair-like conformations, and the $\Delta G^{\ddagger}$ value (27.2 kcal/mol) is 10 kcal/mol lower than that for the intramolecular cycloaddition of **5**.

In summary, we have elucidated the origins of the large reactivity differences in intramolecular nitrone cycloadditions of

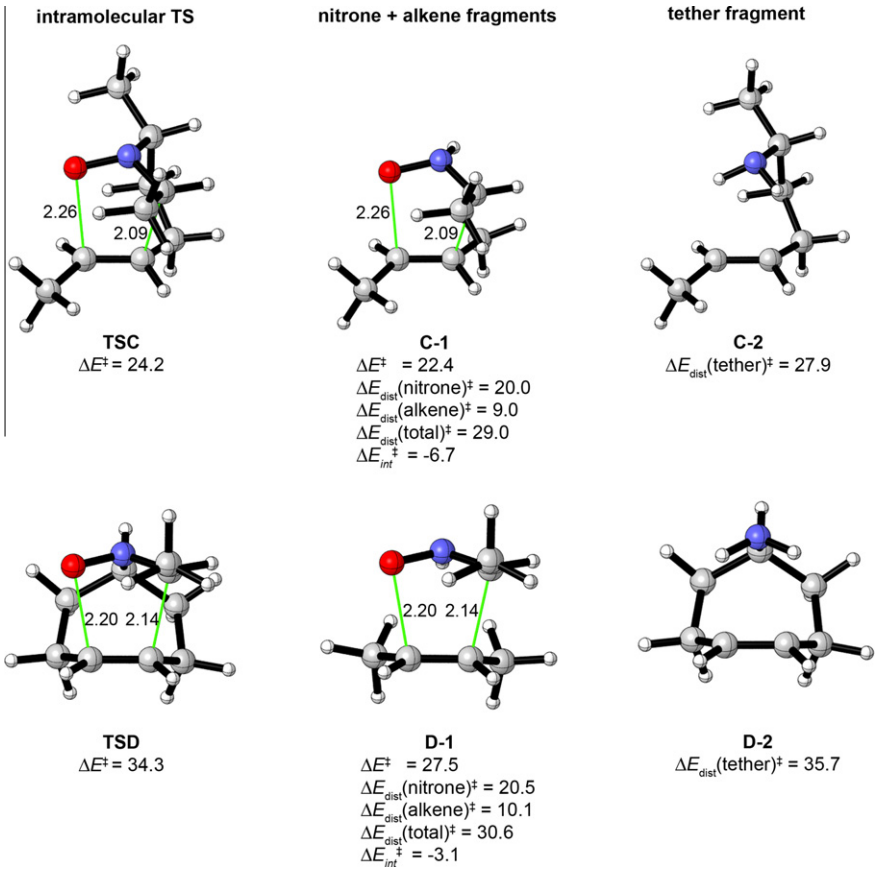

Figure 3. Calculated strain-related energies associated with various fragments of the intermolecular transition structures **TSC** and **TSD**. The structures **C-1** and **D-1** are the structures obtained after removing the atoms connecting the nitrone to the butene component of the alkene (replacing unfilled valences with H). The structures **C-2** and **D-2** represent the geometry of the tether(s) at the TS, and were obtained by replacing the nitrone with an NH_2 group. The bond lengths, angles, and dihedrals of the added H atoms were allowed to relax, but all other structural features were held at the same values as in **TSC** or **TSD**.

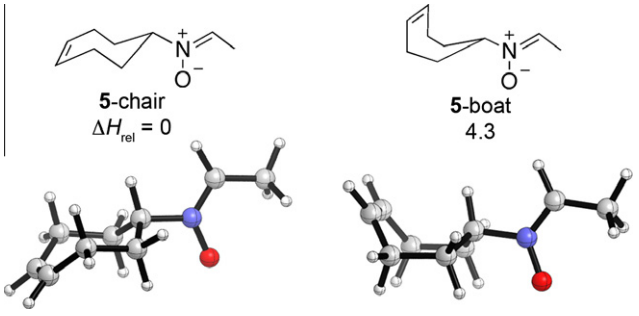

Figure 4. Chair and boat conformations of cycloheptenyl nitrone **5**.

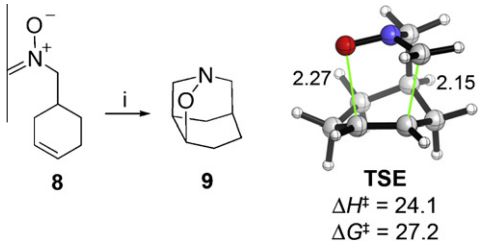

Scheme 2. Oppolzer's 1,3-dipolar cycloaddition of the cyclohexenylmethyl nitrone **8**. Reagents and conditions: (i) toluene, reflux, 9 h, 64%.

several reactant classes. Whereas the single tether in **2** introduces little strain, it does provide a very large entropy advantage, lowering the barrier by 6.9 kcal/mol versus the acyclic analog. By contrast, the cyclic reactant, **5**, achieves an even larger entropic advantage, but the reaction does not occur because of prohibitive tether strain.

Acknowledgments

We thank the NSF (CHE-0548209 to K.N.H.), the Australian Research Council (DP0985623 to E.H.K.), the EPSRC and Fisons Pharmaceuticals plc (CASE studentship to J.T.), and CSIRO (Fellowship to A.B.H.) for generous financial support, and the NCSA, UCLA ATS (USA) and NCI NF (Australia) for computer resources. E.H.K. thanks the ARC Centre of Excellence for Free Radical Chemistry and Biotechnology for generous financial support.

Supplementary data

Supplementary data (the preparation and intramolecular dipolar cycloaddition studies of **5**, all B3LYP geometries and energies, and M06-2X energies for selected species) associated with this article can be found, in the online version, at doi:10.1016/j.tetlet.2010.11.121.

References and notes

1. For a review: Martin, J. N.; Jones, R. C. F. In *Synthetic Applications of 1,3-Dipolar Cycloaddition Chemistry Toward Heterocycles and Natural Products*; Padwa, A., Pearson, W. H., Eds.; Wiley: Hoboken, 2003; pp 1–82.

2. (a) Davison, E. C.; Holmes, A. B.; Forbes, I. T. *Tetrahedron Lett.* **1995**, *36*, 9047–9050; (b) Davison, E. C.; Forbes, I. T.; Holmes, A. B.; Warner, J. A. *Tetrahedron* **1996**, *52*, 11601–11624; For a review: (c) Holmes, A. B.; Bourdin, B.; Collins, I.; Davison, E. C.; Rudge, A. J.; Stork, T. C.; Warner, J. A. *Pure Appl. Chem.* **1997**, *69*, 531–536.
3. (a) LeBel, N. A.; Balasubramanian, N. *J. Am. Chem. Soc.* **1989**, *111*, 3363–3368; (b) Williams, G. M.; Roughley, S. D.; Davies, J. E.; Holmes, A. B.; Adams, J. P. *J. Am. Chem. Soc.* **1999**, *121*, 4900–4901; (c) Davison, E. C.; Fox, M. E.; Holmes, A. B.; Roughley, S. D.; Smith, C. J.; Williams, G. M.; Davies, J. E.; Raithby, P. R.; Adams, J. P.; Forbes, I. T.; Press, N. J.; Thompson, M. J. *J. Chem. Soc., Perkin Trans. 1* **2002**, 1494–1514; (d) Smith, C. J.; Holmes, A. B.; Press, N. J. *Chem. Commun.* **2002**, 1214–1215; (e) Horsley, H. T.; Holmes, A. B.; Davies, J. E.; Goodman, J. M.; Silva, M. A.; Pascu, S. I.; Collins, I. *Org. Biomol. Chem.* **2004**, *2*, 1258–1265; (f) Brasholz, M.; Macdonald, J. M.; Saubern, S.; Ryan, J. H.; Holmes, A. B. *Chem. Eur. J.* **2010**, *16*, 11471–11480.
4. Holmes, A. B.; Swithenbank, C.; Williams, S. F. *J. Chem. Soc., Chem. Commun.* **1986**, 265–266.
5. GAUSSIAN 03, Revision C.02, Frisch, M. J.; Trucks, G. W.; Schlegel, H. B.; Scuseria, G. E.; Robb, M. A.; Cheeseman, J. R.; Montgomery, J. A., Jr.; Vreven, T.; Kudin, K. N.; Burant, J. C.; Millam, J. M.; Iyengar, S. S.; Tomasi, J.; Barone, V.; Mennucci, B.; Cossi, M.; Scalmani, G.; Rega, N.; Petersson, G. A.; Nakatsuji, H.; Hada, M.; Ehara, M.; Toyota, K.; Fukuda, R.; Hasegawa, J.; Ishida, M.; Nakajima, T.; Honda, Y.; Kitao, O.; Nakai, H.; Klene, M.; Li, X.; Knox, J. E.; Hratchian, H. P.; Cross, J. B.; Bakken, V.; Adamo, C.; Jaramillo, J.; Gomperts, R.; Stratmann, R. E.; Yazyev, O.; Austin, A. J.; Cammi, R.; Pomelli, C.; Ochterski, J. W.; Ayala, P. Y.; Morokuma, K.; Voth, G. A.; Salvador, P.; Dannenberg, J. J.; Zakrzewski, V. G.; Dapprich, S.; Daniels, A. D.; Strain, M. C.; Farkas, O.; Malick, D. K.; Rabuck, A. D.; Raghavachari, K.; Foresman, J. B.; Ortiz, J. V.; Cui, Q.; Baboul, A. G.; Clifford, S.; Cioslowski, J.; Stefanov, B. B.; Liu, G.; Liashenko, A.; Piskorz, P.; Komaromi, I.; Martin, R. L.; Fox, D. J.; Keith, T.; Al-Laham, M. A.; Peng, C. Y.; Nanayakkara, A.; Challacombe, M.; Gill, P. M. W.; Johnson, B.; Chen, W.; Wong, M. W.; Gonzalez, C.; Pople, J. A. Gaussian, Inc., Wallingford CT, 2004.
6. (a) Cossío, F. P.; Morao, I.; Jiao, H.; Schleyer, P. v. R. *J. Am. Chem. Soc.* **1999**, *121*, 6737–6746; (b) Di Valentin, C.; Freccero, M.; Gandolfi, R.; Rastelli, A. *J. Org. Chem.* **2000**, *65*, 6112–6120; (c) Silva, M. A.; Goodman, J. M. *Tetrahedron* **2002**, *58*, 3667–3671; (d) Herrera, R.; Nagarajan, A.; Morales, M. A.; Méndez, F.; Jiménez-Vázquez, H. A.; Zepeda, L. G.; Tamariz, J. *J. Org. Chem.* **2001**, *66*, 1252–1263; (e) Domingo, L. R. *Eur. J. Org. Chem.* **2000**, 2265–2272; (f) Magnuson, E. C.; Pranata, J. *J. Comput. Chem.* **1998**, *19*, 1795–1804; (g) Ess, D. H.; Houk, K. N. *J. Am. Chem. Soc.* **2007**, *129*, 10646–10647; (h) Ess, D. H.; Houk, K. N. *J. Am. Chem. Soc.* **2008**, *130*, 10187–10198.
7. In **TSB**, the nitrone *C*-methyl group is on the opposite side of the forming five-membered ring from the butene methyl groups. This TS is 0.5 kcal/mol higher in energy ($\Delta\Delta H^{\ddagger}$) than the TS where the *C*-methyl group is on the same side as the butene methyl groups, but is a better model for the arrangement of groups in **TSD**.
8. (a) Huisgen, R.; Sturm, H.-J.; Wagenhofer, H. *Z. Naturforsch., B* **1962**, *17*, 202–203; (b) Huisgen, R. *Angew. Chem., Int. Ed. Engl.* **1963**, *2*, 633–645; (c) Huisgen, R.; Seidl, H.; Brüning, I. *Chem. Ber.* **1969**, *102*, 1102–1116.
9. (a) Zhao, Y.; Truhlar, D. G. *Theor. Chem. Acc.* **2008**, *120*, 215–241; (b) Zhao, Y.; Truhlar, D. G. *Acc. Chem. Res.* **2008**, *41*, 157–167.
10. M06-2X calculations were performed in GAUSSIAN 09: Frisch, M. J.; Trucks, G. W.; Schlegel, H. B.; Scuseria, G. E.; Robb, M. A.; Cheeseman, J. R.; Scalmani, G.; Barone, V.; Mennucci, B.; Petersson, G. A.; Nakatsuji, H.; Caricato, M.; Li, X.; Hratchian, H. P.; Izmaylov, A. F.; Bloino, J.; Zheng, G.; Sonnenberg, J. L.; Hada, M.; Ehara, M.; Toyota, K.; Fukuda, R.; Hasegawa, J.; Ishida, M.; Nakajima, T.; Honda, Y.; Kitao, O.; Nakai, H.; Vreven, T.; Montgomery, J. A., Jr.; Peralta, J. E.; Ogliaro, F.; Bearpark, M.; Heyd, J. J.; Brothers, E.; Kudin, K. N.; Staroverov, V. N.; Kobayashi, R.; Normand, J.; Raghavachari, K.; Rendell, A.; Burant, J. C.; Iyengar, S. S.; Tomasi, J.; Cossi, M.; Rega, N.; Millam, N. J.; Klene, M.; Knox, J. E.; Cross, J. B.; Bakken, V.; Adamo, C.; Jaramillo, J.; Gomperts, R.; Stratmann, R. E.; Yazyev, O.; Austin, A. J.; Cammi, R.; Pomelli, C.; Ochterski, J. W.; Martin, R. L.; Morokuma, K.; Zakrzewski, V. G.; Voth, G. A.; Salvador, P.; Dannenberg, J. J.; Dapprich, S.; Daniels, A. D.; Farkas, Ö.; Foresman, J. B.; Ortiz, J. V.; Cioslowski, J.; Fox, D. J. GAUSSIAN 09, Revision A.02, Gaussian, Inc., Wallingford CT, 2009.
11. Values of $\Delta H^{\ddagger}$ at 0 K, calculated from the M06-2X single-point electronic energies in conjunction with the B3LYP zero-point energies. The B3LYP/6-31G(d) values of $\Delta H^{\ddagger}$ at this temperature are 24.9 and 34.7 kcal/mol for **TSC** and **TSD**, respectively. Use of M06-2X with the 6-31G(d) basis set provided somewhat lower activation energies. Details are provided in the Supplementary data.
12. Replacement of the deleted atoms by Me groups rather than H atoms may have provided a better model, but the constrained structures possessed imaginary vibrational frequencies. The fully-optimized TSs corresponding to **C-1** and **D-1** are geometrically similar to **TSA** and **TSB**.
13. Oppolzer, W.; Siles, S.; Snowden, R. L.; Bakker, B. H.; Petrzilka, M. *Tetrahedron* **1985**, *41*, 3497–3509.